ORIGINAL RESEARCH

Impact of Cholesterol Metabolism on H_2O_2-Induced Oxidative Stress Injury in HepG2 Cells Treated with Fatty Acids

Qiao Tang, PG; Li Du, MD; Qian Sun, PhD

ABSTRACT

Objective • This study aimed to evaluate the expression of genes involved in cholesterol metabolism and establish their association with oxidative stress (OS).

Methods • We employed an *in vitro* experimental design and cells were divided into six groups: C (control), CH (HepG2 + H_2O_2), CHN (HepG2 + H_2O_2 + NAC), F (FFA-treated HepG2), FH (FFA-treated HepG2 + H_2O_2), and FHN (FFA-treated HepG2 + H_2O_2 + NAC). Cell viability was assessed using the MTT assay, while successful FFA model establishment was confirmed via Oil Red staining and absorbance. Oxidative stress injury was gauged by measuring ROS, SOD activity, and MDA content. RNA transcription and protein expression of cholesterol-related (*DHCR24*, *DHCR7*) and oxidative stress-related (*NFE2L2*, *HMOX1*) genes were also examined via RT-qPCR and WB.

Results • The impact of H_2O_2 on cell viability exhibited a time-dose-dependent pattern, paralleling the changes in reactive oxygen species (ROS) levels. Compared to the C group, FFA treatment led to an increase in Oil Red absorption and MDA content and decreased SOD activity.

However, it did not result in a significant reduction in cell viability. The FH group exhibited reduced cell viability and SOD activity, along with a further elevation in MDA content compared to the F group. Furthermore, the increased SOD activity and decreased MDA content observed in the CH group were effectively reversed following NAC treatment. Such a reversal was not evident between the FHN and FH groups. Compared to the control group, genes associated with cholesterol metabolism and oxidative stress (OS) displayed heightened expression levels in the other treatment groups, with the FHN group showing lower expression levels than the FH group. Notably, changes in the protein expressions of *DHCR24*, *DHCR7*, *NFE2L2*, and *HMOX1* were consistent and exhibited correlations.

Conclusions • Cholesterol metabolism emerges as a potential mechanism underlying H_2O_2-induced oxidative stress injury in HepG2 cells treated with FFA. (*Altern Ther Health Med.* 2024;30(1):396-402).

Qiao Tang, PG; Li Du, MD; Qian Sun, PhD; Department of Anesthesiology, Renmin Hospital of Wuhan University, Wuhan, China.

Corresponding author: Qian Sun, PhD
E-mail: queenie_sun@whu.edu.cn

INTRODUCTION

Nonalcoholic fatty liver disease (NAFLD) is a primary reason for liver transplants and is characterized by excessive triglyceride deposition and hepatocyte steatosis.[1] The major factors contributing to NAFLD susceptibility include the direct cytotoxicity of surplus fatty acids, oxidative stress (OS), and lipid peroxidation.[2] The accumulation of free fatty acids (FFA) exceeding mitochondrial β-oxidation capacity leads to reactive oxygen species (ROS) production, intensifying lipid peroxidation and generating harmful reactive metabolites.[3] This process also inflicts damage on mitochondrial DNA and the respiratory chain, disrupting mitochondrial function and subsequently inhibiting lipid β-oxidation, creating a detrimental cycle.[4]

Previous experimental studies have demonstrated that during transplantation, ischemia and reperfusion (IR) can exacerbate irreversible damage in fatty liver (FL), significantly reducing graft survival.[5,6] In the context of FL or IR, nuclear factor erythroid 2-related factor 2 (*NFE2L2* or *Nrf2*) relocates from the cytoplasm to the nucleus, where it binds to the antioxidant response element (ARE), subsequently activating the transcription of antioxidant enzyme genes, such as superoxide dismutase (SOD) and heme oxygenase-1 (*HMOX1* or *HO-1*).[7,8]

Furthermore, studies have demonstrated an increase in the expression of 24-dehydrocholesterol reductase (*DHCR24*) in cells exposed to H_2O_2.[9] Several studies have indicated that *DHCR24* overexpression elevates Akt phosphorylation levels, effectively inhibiting H_2O_2-induced OS and apoptosis.[10,11] Hence, we propose the hypothesis that ROS upregulates *DHCR24* expression, subsequently mitigating H_2O_2-induced OS through the Nrf2/ARE pathway in FFA-treated HepG2 cells.

N-acetylcysteine (NAC) shows promise in improving NAFLD by reducing OS and inflammatory mediators, primarily by elevating intracellular glutathione levels.[12] In various IR models, NAC has been found to mitigate liver damage due to its antioxidant and anti-inflammatory properties.[13] However, limited studies have explored NAC's potential support for FL against IR injury. Giuseppe et al.[14] observed that NAC could confer resistance to IR injury in FL, but its protective effects were more pronounced during the late reperfusion stage in white rabbits fed high-cholesterol diets, showing less impact at the early stage.

IR is a critical factor contributing to adverse outcomes in liver transplantation, with FL, being particularly vulnerable to IR-related damage. This heightened sensitivity creates significant challenges in clinical practice. While pre-administered blood and antioxidants can enhance FL's tolerance to IR to some extent, most Chinese and foreign studies primarily concentrate on normal liver responses to IR, leaving a gap in our understanding of IR-induced damage mechanisms specific to FL.

Therefore, we employed HepG2 cells treated with FFA to create a lipid accumulation model, simulating FL, and exposed them to H_2O_2-induced OS to simulate IR. This approach aims to unravel the molecular mechanisms underlying FL's susceptibility to IR injury and identify potential therapeutic targets for mitigating adverse outcomes in FL transplantation.

MATERIALS AND METHODS

Study Design

This research employs an *in vitro* approach utilizing HepG2 cells to establish a model simulating FL and IR-induced OS. The study aims to uncover the molecular mechanisms underlying FL's susceptibility to IR injury and identify potential therapeutic targets for improving outcomes in FL transplantation.

HepG2 Cells Culture

The human hepatoblastoma cell line, HepG2, was procured from the Chinese Academy of Sciences Cell Bank and maintained in Dulbecco's Modified Eagle Medium/High Glucose (Hyclone, Logan, UT) supplemented with 10% fetal bovine serum (FBS) and 1% penicillin/streptomycin in a 37°C incubator with 5% CO_2. Upon reaching 80% confluence, cells were detached using PBS and 0.25% trypsin (Hyclone, Logan, UT). All experiments were conducted in triplicate, with each experiment repeated three times.

Cell Seeding and Grouping

HepG2 cells (4×10^5 per well) were seeded in 24-well plates and incubated overnight at 37°C. They were then categorized into six groups as follows: (1) Control Group (C group): treated without FFA, H_2O_2, and NAC; (2) H_2O_2 Group (CH group): treated with H_2O_2 only; (3) H_2O_2 + NAC Group (CHN group) - treated with H_2O_2 and NAC; (4) FFA Group (F group) - treated with FAA only; (5) FAA + H_2O_2 Group (FH group) -

treated with FAA and H_2O_2; (6) FAA + H_2O_2 + NAC Group (FHN group) - treated with FAA, H_2O_2, and NAC.

MTT Assay

HepG2 cells were seeded at a density of 1×10^5 cells per well in a 96-well plate and cultured in DMEM containing varying concentrations of H_2O_2 (0, 100, 200, 400, 800, and 1000 μM) from Sigma-Aldrich; Merck KGaA, Germany. After exposure for 1, 2, and 4 hours,[15-17] 0.8 mg/ml MTT was added to each well and incubated at 37°C in a 5% CO_2 atmosphere for 4 hours. The formazan crystals were then dissolved in serum-free medium. Following a PBS wash, 1 ml of DMSO was added to each well and gently shaken for 10 minutes to ensure complete dissolution. The resulting solution was evenly transferred to another 96-well plate, and absorbance at 560 nm was measured using a Microporous Plate Spectrophotometer system (Spectra max190 Molecular Devices). Data analysis was performed using SoftMax Pro software (version 2.2.1), and the results were expressed as a percentage of the control values.

ROS Assay

HepG2 cells were seeded at a density of 1×10^5 cells per well in a 96-well plate and exposed to DMEM containing varying concentrations of H_2O_2 (0, 100, 200, and 400 μM). After a 2-hour incubation, the cells were treated with 20 μM 2',7'-dichlorofluorescin diacetate (DCFH-DA, from Sigma-Aldrich; Merck KGaA, Germany) at 37°C for 1 hour in a dark environment. Subsequently, the cells were washed with PBS, and ROS production was quantified using an LSRII flow cytometer and FACS Diva software (Becton Dickinson). The resulting data were analyzed using FlowJo software version 7.6.1 (FlowJo LLC, Ashland, OR, USA).

Treatment with Free Fatty Acid (FFA) Mixtures

To prepare 10 mM stock solutions of FFA mixtures, free-fatty acid-bound Bovine Serum Albumin (BSA) was mixed with 5 mM palmitic acid (PA)/BSA (Cat. no.: 57-10-3 and 9048-46-8, Sigma-Aldrich; Merck KGaA, Germany) and 5 mM oleic acid (OA)/BSA (Cat. no.: A6003, Sigma Aldrich; Merck KGaA, Germany) at a 1:1 ratio for 1 hour at 37°C. HepG2 cells (4×10^5 cells per well) were seeded in 24-well plates and divided into two groups. One group was incubated in DMEM with the vehicle, while the other was treated with 0.5 mM FFA for 24 hours.

Oil Red Staining and Semi-quantification

The oil red working solution was prepared by dissolving 0.5 mg/mL oil red in a mixture of isopropanol and water in a 3:2 volume ratio. HepG2 cells were fixed with formalin, washed with PBS, and stained for 15 minutes. The stained cells were observed directly under a light microscope (Olympus, Tokyo, Japan). For semi-quantitative analysis of lipid content, 100% isopropanol was added, followed by 5 minutes of agitation. The optical density was then measured at 492 nm using a microplate reader (Victor3 1420-050; Perkin Elmer).

Measurement of SOD Activity and MDA Content

Following treatment with PBS and sonication, HepG2 cell proteins were quantified using the bicinchoninic acid (BCA) method. SOD activity and MDA content were assessed using chemical kits (Cat. no. A00132 and A00312, respectively; Nanjing Jiancheng Biochemicals Ltd., China). SOD activity was expressed as U/mg protein, while MDA content was reported in nmol/mg protein. One unit of enzyme activity was defined as the amount that inhibited 50% of pyrogallol autooxidation.

Real-Time Reverse Transcription-Polymerase Chain Reaction (RT-qPCR) Analysis

Total RNA extraction from cells was performed using TRIzol reagent (Thermo Fisher Scientific), and cDNA preparation was carried out using the QuantiTect Reverse Transcription Kit (Cat. No. 205310, QIAGEN, Germany). RT-qPCR reactions were conducted on an iCycler Real-Time Detection System (Bio-Rad Laboratories, Inc., USA) using iQ SYBR Green Supermix. The expression levels of target mRNA sequences were determined using the $2^{-\Delta\Delta Ct}$ method, normalized to β-actin. Primer sequences are provided in Table 1.

Western Blotting Assay

RIPA Lysis and Extraction Buffer were added to the harvested cells, supplemented with a protease and phosphatase inhibitor cocktail (Cat. no. 89900 and 78428, Thermo Fisher Scientific, Inc., USA). Total protein extracts were quantified using the BCA method. After electrophoresis, a 30-μg protein sample separated by 10% SDS-PAGE was transferred onto a polyvinylidene fluoride membrane. The membrane was blocked with 5% skim milk for 1 hour at room temperature and then incubated overnight with primary antibodies (anti-GAPDH, anti-DHCR24, anti-DHCR7, anti-NFE2L2, anti-HMOX1) at 4°C.

Following PBS washing, the membrane was probed with horseradish peroxidase-conjugated goat anti-rabbit IgG secondary antibodies (Cat. no. sc2357; Santa Cruz Biotechnology, Inc.; 1:2000). Protein bands were visualized using the enhanced chemiluminescence system (ECL) Select™ Western Blotting Detection Reagent (Cat. no. RPN2235, GE Amersham Biosciences, USA) and captured using the iBright™ FL1500 Imaging System (Thermo Fisher Scientific, Inc., USA). Band intensities were quantified using ImageJ Software version 1.6 (National Institutes of Health, Bethesda, MD, USA).

Statistical Analysis

Data are presented as mean values ± standard deviation ($\bar{x} \pm s$). Statistical analysis was conducted using GraphPad Prism statistical software (GraphPad Software, Inc., La Jolla, CA, USA). To determine statistical significance between two groups, an unpaired two-tailed Student's t test was applied. For comparisons among more than two groups, one-way/two-way ANOVA was employed, followed by Tukey's post hoc test for multiple-group comparisons. All experiments and assays were independently replicated a minimum of three times. Statistical significance was considered at $P < .05$.

Table 1. Gene-Specific Primers Used for Real-Time RT-PCR.

Genes	Forword (→)	Reverse (→)
DHCR24	AGTCCAGTTCCCCGTTTA	CTTACCCAGCACCTTCAA
DHCR7	GCAGGGGTTGTGAACAAGTAT	GAGACGGCATAGCCAAGGAT
HMGCR	GTCATTCCAGCCAAGGTTGT	GGGACCACTTGCTTCCATTA
HMGCS1	CATTAGACCGCTGCTATTCTGTC	TTCAGCAACATCCGAGCTAGA
LDLR	GTGCTCCTCGTCTTCCTTTG	TAGCTGTAGCCGTCCTGGTT
NFE2L2	GCTCAACTTGCATTAATTCGGG	TCAGTAGGTGAAGGCTTTTCTC
HMOX1	TCTTCACCTTCCCCAACATTG	CTCTGGTCCTTGGTGTCATG
GSTA1	CTGCCCGTATGTCCACCTG	AGCTCCTCGACGTAGTAGAGA
GSTA2	TGAGGAACAAGATGCCAAGC	CAGAGGGAAGCTGGAAATAAGG
β-actin	CATGTACGTTGCTATCCAGGC	CTCCTTAATGTCACGCACGAT

Note: *DHCR24*: a gene encoding "24-dehydrocholesterol reductase." This enzyme plays a role in cholesterol biosynthesis. *DHCR7*: a gene encoding " dehydrocholesterol reductase." It is involved in the conversion of 7-dehydrocholesterol to cholesterol in cholesterol biosynthesis. *HMGCR*: gene encoding "3-hydroxy-3-methylglutaryl-coenzyme A reductase," a key enzyme in cholesterol synthesis. *HMGCS1*: gene encoding "3-hydroxy-3-methylglutaryl-coenzyme A synthase 1," enzyme involved in cholesterol synthesis. *LDLR*: gene encoding "Low-Density Lipoprotein Receptor," which plays a crucial role in regulating cholesterol levels in the body. *NFE2L2*: the gene encoding "Nuclear Factor, Erythroid 2 Like 2" (also known as Nrf2), a transcription factor involved in the regulation of antioxidant and cytoprotective genes. *HMOX1*: gene encoding "Heme Oxygenase 1," an enzyme that breaks down heme into biliverdin, which has antioxidant properties. *GSTA1* and *GSTA2*: genes encoding "Glutathione S-Transferase Alpha 1" and "Glutathione S-Transferase Alpha 2," enzymes involved in detoxification and antioxidant processes. *β-actin*: a reference gene for normalization in real-time RT-PCR experiments. It represents "Beta-actin," a commonly used reference gene for gene expression analysis.

**Figure 1.** H_2O_2-Induced Oxidative Stress Injury in HepG2 Cells
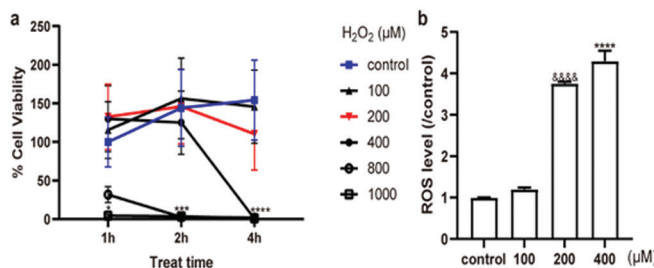
Note: Figure 1 shows the impact of H_2O_2 on HepG2 cells. (a) The cell viability of HepG2 cells exposed to different concentrations of H_2O_2 over various durations demonstrates a time-dose-dependent response. (b) Measurement of intracellular ROS levels in HepG2 cells treated with varying H_2O_2 concentrations for 2 hours relative to the control group (0 μM H_2O_2). Data are presented as ($\bar{x} \pm s$). *$P < .05$ indicates statistical significance compared to the control group at 1000 μM; ***$P < .001$ compared to the control group at 800 or 1000 μM; ****$P < .0001$ compared to the control group at 400, 800, or 1000 μM; $^{\&\&\&\&}P < .0001$ compared to the control group at 200 μM.

RESULTS

### H_2O_2-Induced Time-Dose Dependent Cell Injury

To evaluate the impact of H_2O_2 on HepG2 cell viability, cells were exposed to varying concentrations of H_2O_2 for different durations (1, 2, and 4 hours). In Figure 1a, compared to the control group (0 μM), cell viability exhibited a significant decline in the 800 and 1000 μM groups after 1 hour, as well as in the 400 and 200 μM groups after 4 hours ($P < .05$). At the 2-hour timepoint, there was no significant difference in cell activity between the 100, 200, and 400 μM H_2O_2 groups and the control group. This observation led to the selection of the 2-hour timepoint for subsequent H_2O_2 exposure study.

Tang— DHCR24-Mediated NRF2/ARE Pathway in FFA-HEPG2 Cells

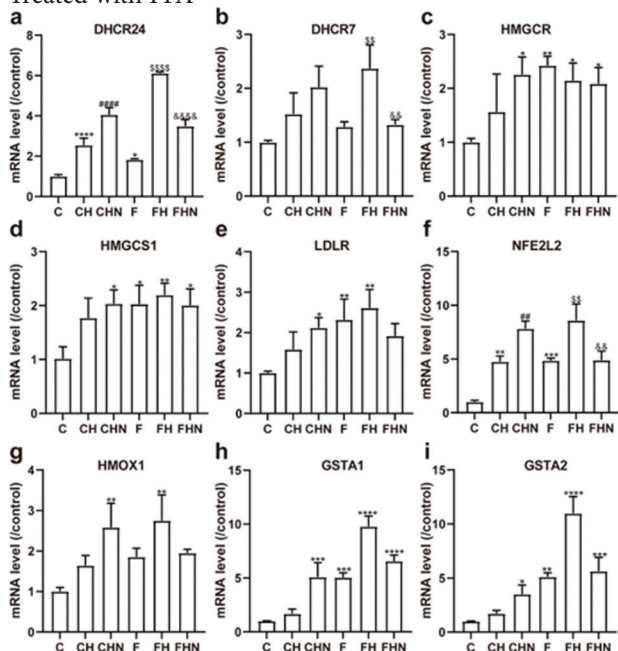**Figure 2.** Establishment of a Lipid Accumulation Model in HepG2 Cells
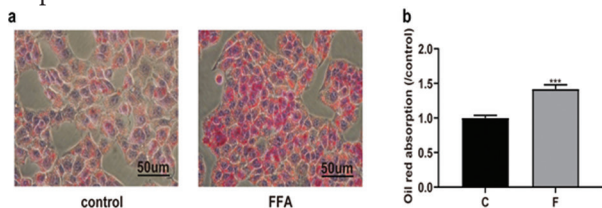
Note: Figure 2 illustrates the successful establishment of a lipid accumulation model in HepG2 cells. (a) Representative photomicrographs of HepG2 cells stained with oil red, showing lipid accumulation, with and without FFA treatment (original magnification, × 400). (b) Quantitative analysis of lipid accumulation through oil red absorption relative to the control group. Data are presented as ($\bar{x} \pm s$). ***$P < .001$ compared to the control group.

Figure 3. H_2O_2-Induced Injury in FFA-Treated HepG2 Cells
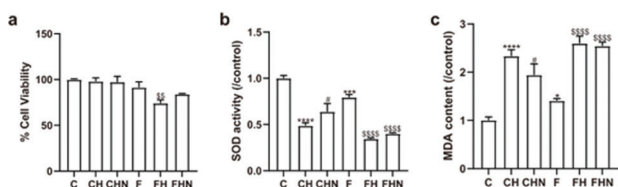
Note: Figure 3 illustrates the impact of H_2O_2-induced injury in HepG2 cells treated with FFA. (a) Cell viability, (b) SOD activity, and (c) MDA content are presented relative to the control group. Data are depicted as ($\bar{x} \pm s$). *$P < .05$, ***$P < .001$, ****$P < .0001$ compared to the control group; #$P < .05$, compared to the CH group; $$P < .01$, $$$$P < .0001$ compared to the F group.

Figure 4. Gene Transcriptions of Cholesterol Metabolism and Oxidative Stress Pathways in H_2O_2-Induced HepG2 Cells Treated with FFA

Note: Figure 4 presents mRNA levels relative to the control group for cholesterol metabolism-related genes: (a) DHCR24, (b) DHCR7, (c) HMGCR, (d) HMGCS1, and (e) LDLR, as well as OS-related genes: (f) NFE2L2, (g) HMOX1, (h) GSTA1, and (i) GSTA2. β-actin served as the housekeeping control. Data are represented as means ± SD ($\bar{x} \pm s$). *$P < .05$, **$P < .01$, ***$P < .001$, ****$P < .0001$ compared to the control group; ##$P < .01$, ####$P < .0001$ compared to the CH group; $$P < .01$, $$$$P < .0001$ compared to the F group; &&$P < 0.01$, &&&&$P < .0001$ compared to the CH group.

Dependence of Intracellular ROS Levels on H_2O_2 Concentration

To assess the extent of H_2O_2-induced OS, intracellular ROS levels were quantified using flow cytometry. The flow cytometry analysis revealed that ROS levels in the 200 and 400 µM groups significantly exceeded those in the control and 100 µM groups. Intracellular ROS levels in response to 200 and 400 µM H_2O_2 exhibited 3.8- and 4.3-fold increases relative to the control group, respectively ($P < .05$, Figure 1b). Consequently, it was inferred that treatment with 200 µM H_2O_2 for 2 hours induced intracellular OS without inducing cell death, making it suitable for subsequent experimental modeling.

Establishment of the Lipid Accumulation Model

Following 24 hours of FFA treatment, the density and size of the red areas representing lipid droplets in HepG2 cells increased (Figure 2a). Significantly greater oil red absorption was observed in the FFA group compared to the control group, confirming the successful establishment of the lipid accumulation model in HepG2 cells ($P < .05$, Figure 2b).

Enhanced H_2O_2-Induced Injury in FFA-Treated HepG2 Cells

We conducted assessments of cell viability and OS indices to determine the extent of H_2O_2-induced injury in FFA-treated HepG2 cells. There were no significant differences in cell viability among the C, CH, CHN, and F groups, while viability decreased notably in the FH and FHN groups (Figure 3a). Compared to the C group, SOD activity decreased, and MDA content increased in both the CH and F groups, with these effects being reversed by NAC in the CHN group relative to the CH group ($P < .05$, Figure 3b). Interestingly, the differences between the FHN and FH groups were less pronounced. Overall, H_2O_2-induced injury was increased in FFA-treated HepG2 cells, and NAC did not mitigate this effect.

mRNA Levels of Genes Associated with Cholesterol Metabolism and OS Pathways

To gain further insights into the molecular mechanisms underlying H_2O_2-induced injury in FFA-treated HepG2 cells and the limited protective effect of NAC (Figure 4), we examined the mRNA levels of genes related to cholesterol metabolism and OS. In the CH and F groups, mRNA levels of DHCR24 and DHCR7 increased compared to the C group, which was further accentuated in the CHN and FH groups ($P < .05$).

However, NAC reduced the mRNA levels of DHCR24 and DHCR7 in the FHN group compared to the FH group. Additionally, in the CH, CHN, F, FH, and FHN groups relative to the C group, mRNA levels of HMGCR, HMGCS1, and LDLR exhibited an increase ($P < .05$). The trends in mRNA levels of NFE2L2, HMOX1, GSTA1, and GSTA2 similar to those of DHCR24 and DHCR7 ($P < .05$).

Protein Expression Associated with Cholesterol Metabolism and OS Pathways in FFA-Treated HepG2 Cells

Compared to the C group, protein expressions of DHCR24 and NFE2L2 increased in the CH and F groups, which was further amplified in the CHN and FH groups ($P < .05$, Figure

5). However, notably, NAC decreased protein expressions of *DHCR24* and *NFE2L2* in the FHN group in contrast to the FH group. Apart from protein expressions of *DHCR7* in the F groups and *HMOX1* in the CH group, which did not exhibit an increase compared to the C group, the trends in protein expressions of *DHCR7* and *HMOX1* mirrored those of *DHCR24* and *NFE2L2* in other groups ($P < .05$). It is worth noting that the excessive accumulation of *DHCR24* in FFA-treated cells may lead to the depletion of *NFE2L2*, resulting in an insufficient response to NAC.

DISCUSSION

Oleic and palmitic acids are the most abundant FFAs in hepatic triglyceride patients with fatty liver.[18] By culturing HepG2 cells with appropriate ratios of oleic and palmitic acids, we successfully induced lipid overload, achieving a lipid overaccumulation model similar to hepatocytes in FL patients.[19] In this study, the FFA-treated HepG2 cell model was effectively established for lipid accumulation, and cell viability showed no significant change compared to normal cells without FFA treatment. Furthermore, we assessed the level of OS in HepG2 cells through measurements of SOD activity and MDA content. Our findings revealed that FFA-treated cells exhibited higher OS levels compared to normal cells.

H_2O_2 is a major contributor to intracellular ROS production, capable of permeating various cells and tissues, leading to cellular damage and apoptosis. This damage is characterized by protein and lipid oxidation and the generation of advanced glycation end products.[20] In our study, H_2O_2 induced OS in HepG2 cells. Notably, higher concentrations of H_2O_2 exhibited a more pronounced detrimental effect on the cells as the exposure time increased. Considering cell viability and ROS levels, we selected the treatment of 200 μM H_2O_2 for 2 hours for subsequent experiments. Unlike other concentrations, this concentration and duration provided a stable OS environment without inducing cell death.

In this study, cell viability remained constant in the normal H_2O_2-treated HepG2 cell model, but a significant decline in cell viability was observed in the FFA-treated HepG2 cell model upon H_2O_2 treatment compared to those without H_2O_2 treatment. This observation suggests that the FFA-treated HepG2 cell model exhibits greater sensitivity to OS than normal cells. The susceptibility of FL to IR is further highlighted by the decrease in antioxidant enzymes and the concurrent increase in lipid peroxidation.

Oxidative stress plays a pivotal role in developing and progressing fatty liver and ischemia-reperfusion injury. Extensive research has demonstrated that administering the antioxidant N-acetylcysteine can mitigate FL and IR injuries by inhibiting caspase activation, reducing ROS levels, and elevating total glutathione levels.[21, 22] A recent study further substantiated the beneficial effects of NAC in alleviating IR damage in mice with steatohepatitis. This effect is likely attributed to a combination of antioxidant and anti-inflammatory actions. Interestingly, Nrf2 levels were found to

Figure 5. Protein Expression of Cholesterol Metabolism and Oxidative Stress Pathway in H_2O_2-Induced HepG2 Cells Treated with FFA
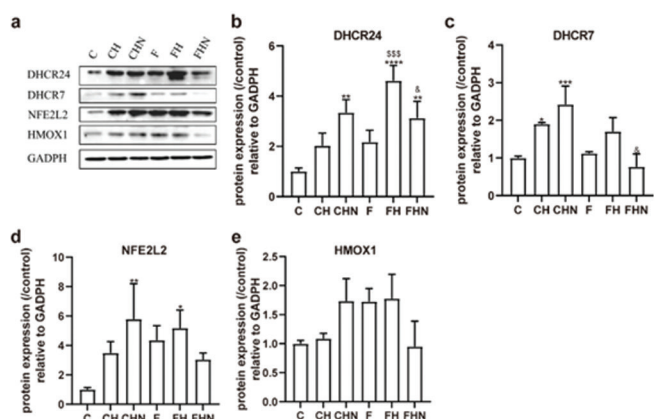
Note: Figure 5 illustrates the protein expressions relative to the control group for (a) *DHCR24*, (b) *DHCR7*, (c) *NFE2L2*, and (d) *HMOX1*. *GADPH* was employed as the housekeeping control. Data are presented as means ± SD ($\bar{x} \pm s$). *$P < .05$, **$P < .01$, ***$P < .001$, ****$P < .0001$ compared to the control group; $^{\$\$\$}P < .001$ compared to the F group, $^{\&}P < .05$ compared to the FH group

be reduced in this context, warranting further investigation.[23]

Additionally, the alterations in cell viability, SOD activity, and MDA content observed in the FFA model treated with H_2O_2 could not be reversed by NAC. This result suggests that the protective effect of NAC on FFA-treated HepG2 cells exposed to H_2O_2 was significantly attenuated in the FFA-induced HepG2 cell model. This finding highlights the need to enhance protection against IR injury in FL through a combination of pharmaceutical agents or methodologies. It is worth noting that we did not investigate the optimal concentration of NAC in FFA-treated HepG2 cells, as excessive NAC may potentially induce cell apoptosis.[24]

NFE2L2 is a redox-regulated transcription factor that can activate various pathways, including an excess of ROS or endoplasmic reticulum stress. It plays a role in improving FL function and preventing deterioration and serves as a protective factor against IR injury.[25] *HMOX1*, a downstream gene regulated by *NFE2L2*, has also been demonstrated to offer protection against FL and IR injury.[26]

Recent studies have shown that antioxidants can mitigate IR damage in FL by activating the *NFE2L2/HMOX1* pathway.[8,27] Interestingly, in normal cells treated with H_2O_2, NAC significantly increased the transcription and expression of hepatic oxidative stress-related genes (*NFE2L2*, *HMOX1*, *GSTA1*, and *GSTA2*). In contrast, the FFA-HepG2 cells showed the opposite response. Overall, it appears that the *NFE2L2/HMOX1* signaling pathway may underlie the reduced protective effect of NAC on FFA-HepG2 cells, possibly due to the depletion of *NFE2L2*.

Current studies have shown that cholesterol metabolism in NAFLD is characterized by increased synthesis and decreased absorption, while LDL cholesterol concentration remains unchanged.[28] One of the mechanisms by which NAFLD progresses to hepatitis is the deterioration of

cholesterol metabolism by affecting the formation of bile acids.[29] Disruption of cholesterol metabolism increases liver disease severity and cardiovascular risk, including increased *HMGCR* for cholesterol synthesis and decreased LDLR for intake, ultimately leading to increased free cholesterol.[30]

Atorvastatin therapy or reduction of cholesterol content through squalene synthase can enhance the tolerance of fatty liver to IR damage.[31] In cholesterol synthesis, *DHCR24* is a widely expressed oxidoreductase residing in the endoplasmic reticulum. It catalyzes the conversion of depot sterols to cholesterol.[32] Cells exposed to H_2O_2 upregulate *DHCR24* gene expression, and the administration of *DHCR24* inhibitors decreases H_2O_2-induced cytotoxicity, suggesting that *DHCR24* exerts a protective effect on OS correlated with ROS scavenging.[33] Another enzyme involved in cholesterol biosynthesis is *DHCR7*, which converts 7-dehydrocholesterol to cholesterol.[34]

We observed that H_2O_2 upregulated both *DHCR24* and *DHCR7* in FFA-HepG2 cells, which was consistent with the increase in *NFE2L2/HMOX1*. However, compared to the FH group, NAC decreased protein expressions of *DHCR24* and *NFE2L2* in the FHN group. Notably, it can be inferred that the excessive accumulation of *DHCR24* in FFA-treated cells leads to the exhaustion of *NFE2L2*, resulting in an insufficient response to NAC.

Study Limitations

Few limitations should be acknowledged in this study. Firstly, the experiments were conducted *in vitro* using HepG2 cells, which may not fully replicate the complex *in vivo* conditions of fatty liver disease and ischemia-reperfusion injury. Additionally, we did not explore the optimal concentration of NAC in FFA-treated HepG2 cells, which could be a potential area for future research. Furthermore, while we focused on the molecular mechanisms involving genes like *NFE2L2*, *DHCR24*, and *DHCR7*, the clinical translation of these findings into therapeutic strategies for fatty liver transplantation requires further investigation. Lastly, the study primarily employed HepG2 cells, and the response may vary in different cell types or animal models. Despite these limitations, this research provides valuable insights into the role of cholesterol metabolism and oxidative stress in fatty liver disease and ischemia-reperfusion injury, paving the way for future studies to explore more comprehensive treatment approaches.

CONCLUSION

In conclusion, our study has achieved several significant findings. We effectively created a lipid accumulation model using FFA, providing a valuable tool for studying the mechanisms underlying fatty liver disease. Importantly, we observed that FFA-treated HepG2 cells displayed heightened sensitivity to oxidative stress, emphasizing the vulnerability of fatty liver to ischemia-reperfusion injury. Notably, our results suggest that the conventional antioxidant NAC may not fully mitigate the impact of oxidative stress in this

context. The pivotal role of *DHCR24* in the *Nrf2/ARE* pathway highlights a potential mechanism contributing to this reduced protective effect of NAC. Moreover, our findings underscore the relevance of cholesterol metabolism-related genes in the context of oxidative stress and fatty liver, potentially opening avenues for novel therapeutic strategies. Overall, this study enhances our understanding of the intricate interplay between oxidative stress, lipid metabolism, and fatty liver disease, offering valuable insights for future research and clinical interventions in the realm of fatty liver transplantation and ischemia-reperfusion injury.

REFERENCES

1. Chalasani N, Younossi Z, Lavine JE, et al. The diagnosis and management of nonalcoholic fatty liver disease: Practice guidance from the American Association for the Study of Liver Diseases. *Hepatology*. 2018;67(1):328-357. doi:10.1002/hep.29367
2. Day CP, James OFW. Steatohepatitis: a tale of two "hits"? *Gastroenterology*. 1998;114(4):842-845. doi:10.1016/S0016-5085(98)70599-2
3. Ockner RK, Kaikaus RM, Bass NM. Fatty-acid metabolism and the pathogenesis of hepatocellular carcinoma: review and hypothesis. *Hepatology*. 1993;18(3):669-676. doi:10.1002/hep.1840180327
4. Ucar F, Sezer S, Erdogan S, Akyol S, Armutcu F, Akyol O. The relationship between oxidative stress and nonalcoholic fatty liver disease: its effects on the development of nonalcoholic steatohepatitis. *Redox Rep*. 2013;18(4):127-133. doi:10.1179/1351000213Y.0000000050
5. El-Badry AM, Moritz W, Contaldo C, Tian Y, Graf R, Clavien PA. Prevention of reperfusion injury and microcirculatory failure in macrosteatotic mouse liver by omega-3 fatty acids. *Hepatology*. 2007;45(4):855-863. doi:10.1002/hep.21625
6. Suzuki T, Yoshidome H, Kimura F, et al. Hepatocyte apoptosis is enhanced after ischemia/reperfusion in the steatotic liver. *J Clin Biochem Nutr*. 2011;48(2):142-148. doi:10.3164/jcbn.10-74
7. Li W, Ma F, Zhang L, et al. S-Propargyl-cysteine Exerts a Novel Protective Effect on Methionine and Choline Deficient Diet-Induced Fatty Liver via Akt/Nrf2/HO-1 Pathway. *Oxid Med Cell Longev*. 2016;2016:4690857. doi:10.1155/2016/4690857
8. Park SW, Kang JW, Lee SM. The role of heme oxygenase-1 in drug metabolizing dysfunction in the alcoholic fatty liver exposed to ischemic injury. *Toxicol Appl Pharmacol*. 2016;292:30-39. doi:10.1016/j.taap.2015.12.025
9. Wu C, Miloslavskaya I, Demontis S, Maestro R, Galaktionov K. Regulation of cellular response to oncogenic and oxidative stress by Seladin-1. *Nature*. 2004;432(7017):640-645. doi:10.1038/nature03173
10. Kuehnle K, Crameri A, Kälin RE, et al. Prosurvival effect of DHCR24/Seladin-1 in acute and chronic responses to oxidative stress. *Mol Cell Biol*. 2008;28(2):539-550. doi:10.1128/MCB.00584-07
11. Yao M, Li F, Xu L, Ma L, Zhang S. 24-Dehydrocholesterol Reductase alleviates oxidative damage-induced apoptosis in alveolar epithelial cells via regulating Phosphatidylinositol-3-Kinase/Protein Kinase B activation. *Bioengineered*. 2022;13(1):155-163. doi:10.1080/21655979.2021.2011634
12. Dludla PV, Nkambule BB, Mazibuko-Mbeje SE, et al. N-Acetyl Cysteine Targets Hepatic Lipid Accumulation to Curb Oxidative Stress and Inflammation in NAFLD: A Comprehensive Analysis of the Literature. *Antioxidants*. 2020;9(12):1283. doi:10.3390/antiox9121283
13. Glantzounis GK, Yang W, Koti RS, Mikhailidis DP, Seifalian AM, Davidson BR. Continuous infusion of N-acetylcysteine reduces liver warm ischaemia-reperfusion injury. *Br J Surg*. 2004;91(10):1330-1339. doi:10.1002/bjs.4694
14. Fusai G, Glantzounis GK, Hafez T, et al. N-Acetylcysteine ameliorates the late phase of liver ischaemia/reperfusion injury in the rabbit with hepatic steatosis. *Clin Sci (Lond)*. 2005;109(5):465-473. doi:10.1042/CS20050081
15. Razali N, Mat Junit S, Ariffin A, Ramli NS, Abdul Aziz A. Polyphenols from the extract and fraction of T. indica seeds protected HepG2 cells against oxidative stress. *BMC Complement Altern Med*. 2015;15(1):438. doi:10.1186/s12906-015-0963-2
16. Deng Y, Ma J, Weng X, et al. Kaempferol-3-O-Glucuronide Ameliorates Non-Alcoholic Steatohepatitis in High-Cholesterol-Diet-Induced Larval Zebrafish and HepG2 Cell Models via Regulating Oxidation Stress. *Life (Basel)*. 2021;11(5):445. doi:10.3390/life11050445
17. He Y, Peng L, Xiong H, et al. The profiles of durian (Durio zibethinus Murr.) shell phenolics and their antioxidant effects on H2O2-treated HepG2 cells as well as the metabolites and organ distribution in rats. *Food Res Int*. 2023;163:163. doi:10.1016/j.foodres.2022.112122
18. Feldstein AE, Canbay A, Guicciardi ME, Higuchi H, Bronk SF, Gores GJ. Diet associated hepatic steatosis sensitizes to Fas mediated liver injury in mice. *J Hepatol*. 2003;39(6):978-983. doi:10.1016/S0168-8278(03)00460-4
19. Gómez-Lechón MJ, Donato MT, Martínez-Romero A, Jiménez N, Castell JV, O'Connor JE. A human hepatocellular in vitro model to investigate steatosis. *Chem Biol Interact*. 2007;165(2):106-116. doi:10.1016/j.cbi.2006.11.004
20. Su, M., et al., *The Antiapoptosis Effect of Glycyrrhizate on HepG2 Cells Induced by Hydrogen Peroxide*. Oxidative Medicine and Cellular Longevity, 2016. **2016**. doi:10.1155/2016/6849758

21. Thong-Ngam D, Samuhasaneeto S, Kulaputana O, Klaikeaw N. N-acetylcysteine attenuates oxidative stress and liver pathology in rats with non-alcoholic steatohepatitis. *World J Gastroenterol*. 2007;13(38):5127-5132. doi:10.3748/wjg.v13.i38.5127

22. Jegatheeswaran S, Siriwardena AK. Experimental and clinical evidence for modification of hepatic ischaemia-reperfusion injury by N-acetylcysteine during major liver surgery. *HPB (Oxford)*. 2011;13(2):71-78. doi:10.1111/j.1477-2574.2010.00263.x

23. Chaves Cayuela N, Kiyomi Koike M, Jacysyn JF, et al. *N*-Acetylcysteine Reduced Ischemia and Reperfusion Damage Associated with Steatohepatitis in Mice. *Int J Mol Sci*. 2020;21(11):4106. doi:10.3390/ijms21114106

24. Alisi A, Piemonte F, Pastore A, et al. Glutathionylation of p65NF-kappaB correlates with proliferating/apoptotic hepatoma cells exposed to pro- and anti-oxidants. *Int J Mol Med*. 2009;24(3):319-326. doi:10.3892/ijmm_00000235

25. Xu D, Xu M, Jeong S, et al. The Role of Nrf2 in Liver Disease: Novel Molecular Mechanisms and Therapeutic Approaches. *Front Pharmacol*. 2019;9:1428. doi:10.3389/fphar.2018.01428

26. Petrtýl J, Dvořák K, Stříteský J, et al. Association of Serum Bilirubin and Functional Variants of Heme Oxygenase 1 and Bilirubin UDP-Glucuronosyl Transferase Genes in Czech Adult Patients with Non-Alcoholic Fatty Liver Disease. *Antioxidants*. 2021;10(12):2000. doi:10.3390/antiox10122000

27. Li S, Takahara T, Fujino M, et al. Astaxanthin prevents ischemia-reperfusion injury of the steatotic liver in mice. *PLoS One*. 2017;12(11):e0187810. doi:10.1371/journal.pone.0187810

28. Simonen P, Kotronen A, Hallikainen M, et al. Cholesterol synthesis is increased and absorption decreased in non-alcoholic fatty liver disease independent of obesity. *J Hepatol*. 2011;54(1):153-159. doi:10.1016/j.jhep.2010.05.037

29. Yan M, Man S, Ma L, Gao W. Comprehensive molecular mechanisms and clinical therapy in nonalcoholic steatohepatitis: an overview and current perspectives. *Metabolism*. 2022;134:155264. doi:10.1016/j.metabol.2022.155264

30. Min H-K, Kapoor A, Fuchs M, et al. Increased hepatic synthesis and dysregulation of cholesterol metabolism is associated with the severity of nonalcoholic fatty liver disease. *Cell Metab*. 2012;15(5):665-674. doi:10.1016/j.cmet.2012.04.004

31. Llacuna L, Fernández A, Montfort CV, et al. Targeting cholesterol at different levels in the mevalonate pathway protects fatty liver against ischemia-reperfusion injury. *J Hepatol*. 2011;54(5):1002-1010. doi:10.1016/j.jhep.2010.08.031

32. Zerenturk EJ, Sharpe LJ, Ikonen E, Brown AJ. Desmosterol and DHCR24: unexpected new directions for a terminal step in cholesterol synthesis. *Prog Lipid Res*. 2013;52(4):666-680. doi:10.1016/j.plipres.2013.09.002

33. Di Stasi D, Vallacchi V, Campi V, et al. DHCR24 gene expression is upregulated in melanoma metastases and associated to resistance to oxidative stress-induced apoptosis. *Int J Cancer*. 2005;115(2):224-230. doi:10.1002/ijc.20885

34. Xiao J, Li W, Zheng X, et al. Targeting 7-Dehydrocholesterol Reductase Integrates Cholesterol Metabolism and IRF3 Activation to Eliminate Infection. *Immunity*. 2020;52(1):109-122.e6. doi:10.1016/j.immuni.2019.11.015